12th IEEE International Conference on Control & Automation (ICCA)
Kathmandu, Nepal, June 1-3, 2016

Integrated Localization System for Autonomous Unmanned Aerial Vehicle Formation Flight

Haibin Duan, *Senior Member, IEEE* and Qinan Luo

Abstract— **This paper presents a formation control framework based on an integrated position sensor system, including two cameras and several inertial sensors, for Unmanned Aerial Vehicles (UAVs) to fly outdoors. A sliding mode controller provides the desired orientation for the UAV to track a desired trajectory. The flight control system takes into account the estimated attitude and position to guide the follower vehicle along trajectories that maintain adequate formation stability. The cameras are employed to detect the relative positions by extracting feature points from specific markers on the UAV. The features are processed to estimate the attitude and position of the follower vehicle. A real-time guidance algorithm is also proposed to merge image measurements with Inertial Measurement Unit (IMU) data for state estimation. The system has been successfully tested in flight experiments, which verify the effectiveness and applicability of the proposed control framework and visual measurement algorithms.**

I. INTRODUCTION

Over the last years, Unmanned Aerial Vehicles (UAVs) and in particular multi-rotor craft is becoming an integral part of future civilian platforms and will be used for complex tasks including surveillance, reconnaissance, precision detection and other cooperative missions [1]. In relation to cooperative missions, more attention is now paid to various control problems associated with multi-UAV moving in formation [2]. Most of the recent works on formation flight has used leader-follower approach, since it is easy to implement. In this structure, one of the UAVs in the formation is designated as the leader, with the rest of the UAVs treated as followers. The basic idea of leader-follower formation control is that the followers receive the entire position and orientation information of the leader, which is related to the certain mission requirements. The common weaknesses as reported in [3]–[4] are that the rear UAV usually exhibits a poorer response than its reference due to the estimation error of relation position. The formation control task is different from pre-defined tracking problem because the follower has to react to the motions of the leader. Therefore, UAVs in formation should have an onboard sensor system to detect relative positions and states.

* This work was partially supported by National Natural Science Foundation of China under grant #61333004, Aeronautical Foundation of China under grant #2015ZA51013, and the Innovation Foundation of BUAA for PhD Graduates.

Haibin Duan is with Bio-inspired Autonomous Flight Systems (BAFS) Research Group, Science and Technology on Aircraft Control Laboratory, School of Automation Science and Electrical Engineering, Beihang University, Beijing, China (e-mail: hbduan@buaa.edu.cn).

Qinan Luo is with Bio-inspired Autonomous Flight Systems (BAFS) Research Group, Science and Technology on Aircraft Control Laboratory, School of Automation Science and Electrical Engineering, Beihang University, Beijing, China (e-mail: qinanluo@buaa.edu.cn).

Many researchers have tried to solve the formation control problem in a variety of methods. For formation control problem, Franchi et al. presented a decentralized system for a groups of UAVs that only relies on relative bearing measurements [5]. Saska developed a navigation and stabilization scheme for 3D heterogeneous formation control [6]. Some other works in formation control implement non-linear model predictive control [7], neural network [8], and high order sliding modes [9].

Recently, studies on onboard vision sensor systems for UAVs have become a challenging interdisciplinary research topic. Such passive and non-cooperative sensors will be very useful wherever Global Positioning System (GPS) is not available due to obstruction or jamming. These characteristics are suitable for three-dimensional guidance in complex and unstructured outdoor environments and also improve the UAV's autonomy and intelligence [10]. In order to complete the formation task, the sensor system is required to provide precise and instant position estimation. There are several approaches to solve this measure problem by using a vision sensor. The early approaches focus on feature extraction and target identification [11]. In addition, several studies utilized a specific visual measurement technique related to geometric and 3D properties of the features, such as feature matching and active contour [12]. Some adaptive observers are proposed to guarantee the stability of the vision sensor and the convergence of the estimators [13]. There is also a comprehensive study on real-time vision-based measurement with an Inertial Measurement Unit (IMU) [14] during aggressive maneuver.

In this work, we describe a formation control framework based on an integrated sensor system, which is employed to sense the relative position and orientation between two UAVs. Since a monocular-vision sensor cannot provide the range information, the binocular stereo vision inspection technique is adopted in our project. The binocular vision sensor measure the relative position by extracting feature points of a specific maker on the UAV. A sliding mode controller provides the desired orientation for the UAV to track a desired trajectory. The proposed framework also exploits the availability of an onboard IMU, for a general position estimator, and for the recovery of the formation trajectory while using visual measurement. The novelty of the approach is that it is able to adapt continuously to complex environmental changes. Being cheap and flexible, multi-rotor helicopter platforms can be developed for many different applications. An octorotor and a quadrotor are intended to serve as platforms for flight experiments and to stuff sensors and other equipment.

The rest of this paper is organized as follows. Section II introduces the UAV model and the design of trajectory

tracking and formation control laws. Section III gives a description of the visual measurement technique for multi-UAV position estimation and the entire formation control framework. The proposed framework is implemented on an octorotor and a quadrotor equipped with the sensor module. Outdoor flight test results are shown and discussed in Section IV, followed by concluding remarks in Section V.

II. Dynamic Modeling and Control Strategy

A. Quadrotor Model

This section describes dynamic model of the follower quadrotor. A quadrotor simply consists of two pairs of rotors, and the motion of the quadrotor can be achieved by controlling the speed of the rotors. The quadrotor position and attitude motion can be described by following 6-DOF equations:

$$\begin{aligned} m\ddot{x} &= (\sin\psi\sin\phi + \cos\psi\cos\phi\sin\theta)T \\ m\ddot{y} &= (-\cos\psi\sin\phi + \sin\psi\sin\phi\sin\theta)T \\ m(\ddot{z}+g) &= \cos\theta\cos\phi T \\ I_{xx}\dot{\omega}_x &= M_x - (I_{zz}-I_{yy})\omega_y\omega_z \\ I_{yy}\dot{\omega}_y &= M_y - (I_{xx}-I_{zz})\omega_x\omega_z \\ I_{zz}\dot{\omega}_z &= M_z \end{aligned} \tag{1}$$

where T presents the total thrust generated from four motors. The roll, pitch and yaw angles (φ, θ, ψ) are mainly produced by the rotors differential thrust. $M_{x,y,z}$ are moments about corresponding axis calculated by the attitude angles. $I_{xx,yy,zz}$ are inertia moments and $w_{x,y,z}$ are rotational velocities. Assume that the attitude stabilization is taken care of by the autopilot, the equations can be simplified as:

$$\begin{aligned} \ddot{x} &= g\theta \\ \ddot{y} &= -g\phi \\ \ddot{z} &= -g + u_1 \end{aligned} \tag{2}$$

where u_1 is the linear acceleration applied to the quadrotor in the z-direction. We use a PID control for attitude stabilization, which can be achieved by using an on-board inertial measurement unit (IMU). The simplified model is valid for small rates of yaw and assume that position of three axes can be controlled independently.

B. Trajectory Tracking Control

The trajectory tracking control strategy, as shown in the block diagram of Fig. 1, is based on the translational dynamics control and provides an acceptable tracking performance to move UAVs to the desired position. A sliding mode controller is adopted in the position control loop.

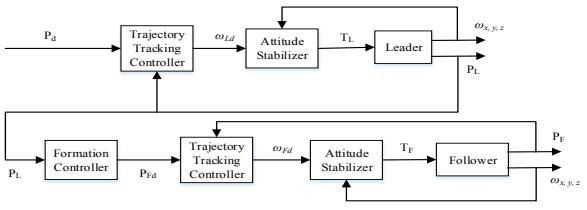

Figure 1. Trajectory tracking control strategy block diagram.

Consider the position vectors $\mathrm{P} = [x\ \mathrm{y}\ \mathrm{z}]^T$ and the position error $\bar{\mathrm{P}} = \mathrm{P} - \mathrm{P}_d$, the trajectory tracking equation can be written as:

$$m\ddot{\bar{\mathrm{P}}} = T\omega - mg\omega - m\ddot{\mathrm{P}}_d \tag{3}$$

Defining the switch function:

$$\sigma_1 = k_1\bar{\mathrm{P}} + k_2\int\bar{\mathrm{P}}dt + \dot{\bar{\mathrm{P}}} \tag{4}$$

where k_1, k_2 are constant control parameters. On the control surface settled by $\sigma_1 = 0$, the error dynamics is:

$$k_1\dot{\bar{\mathrm{P}}} + k_2\bar{\mathrm{P}} + \ddot{\bar{\mathrm{P}}} = 0 \tag{5}$$

By choosing suitable values of parameters k_1 and k_2, an asymptotic convergence of $\bar{\mathrm{P}} \to 0$ can be guaranteed. Despite uncertainties and perturbations, a discontinuity can be added to attract the system dynamics to the surface $\sigma_1 = 0$ and keep it there. Giving the equivalent control as:

$$u_{eq} = [(T\omega)_d]_{eq} = m(g\omega + \ddot{\bar{\mathrm{P}}}_d - k_1\dot{\bar{\mathrm{P}}} - k_2\bar{\mathrm{P}}) \tag{6}$$

Consider the Lyapunov's candidate function by making the assignment:

$$\dot{\sigma}_1 = k_1\dot{\bar{\mathrm{P}}} + k_2\bar{\mathrm{P}} + \frac{1}{m}(T\omega)_d - g\omega - \ddot{\bar{\mathrm{P}}}_d$$

$$V = \frac{1}{2}\sigma_1^T\sigma_1 \tag{7}$$

Differentiating the Lyapunov's function with respect to time and expand the variable $\dot{\sigma}_1$:

$$\dot{V} = \sigma_1^T(k_1\dot{\bar{\mathrm{P}}} + k_2\bar{\mathrm{P}} + \frac{1}{m}(T\omega)_d - g\omega - \ddot{\bar{\mathrm{P}}}_d + \frac{1}{m}\Delta f(\mathrm{P})) \tag{8}$$

Therefore, $\dot{V}$ takes the form

$$\dot{V} = \sigma_1^T(-L_\mathrm{P}\,\mathrm{sgn}(\sigma_1) + \frac{1}{m}\Delta f(\mathrm{P})) \tag{9}$$

$$\dot{V} \le \|\sigma_1\|(-L_\mathrm{P} + \frac{1}{m}t) \tag{10}$$

In the condition of $L_\mathrm{P} \ge \frac{1}{m}t$, $\dot{V}$ will be negative. That means the sliding mode control law solves the trajectory tracking problem, and the desired attitude angles ϕ_d, θ_d can be written as:

$$\phi_d = \arcsin(-\frac{R_{dy} - R_{dx}\tan(\psi_d)}{\sin(\psi_d)\tan(\psi_d) + \cos(\psi_d)}) \tag{11}$$

$$\theta_d = \arcsin(\frac{R_{dx} - \sin(\phi_d)\sin(\psi_d)}{\cos(\phi_d)\cos(\psi_d)}) \tag{12}$$

where $\boldsymbol{R}$ is the rotational matrix from the body frame to the inertial one.

C. Formation Control

In order to maintain the follower quadrotor to a desired relative position from the leader, a formation controller based on sliding mode control is presented. Considering the translational dynamics of the leader-follower formation:

$$\dot{x}_i = v_{ix}\cos(\psi_i) - v_{iy}\sin(\psi_i) \tag{13}$$

$$\dot{y}_i = v_{ix}\sin(\psi_i) + v_{iy}\cos(\psi_i) \tag{14}$$

$$\dot{\psi}_i = \omega_i \tag{15}$$

$$P_x = -(x_L - x_F)\cos(\psi_L) - (y_L - y_F)\sin(\psi_L) \tag{16}$$

$$P_y = (x_L - x_F)\sin(\psi_L) - (y_L - y_F)\cos(\psi_L) \tag{17}$$

$$P_x = P\cos(\varphi) \tag{18}$$

$$P_y = P\sin(\varphi) \tag{19}$$

where x_i, v_{ix}, v_{iy} are position and velocity components of the leader (i=L) and the follower (i=F). w_i are angular velocities for the yaw angle. The relative distance and angle is presented by P and φ (see Fig. 2).

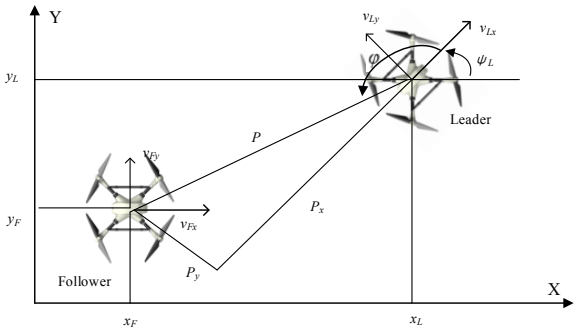

Figure 2. Formation dynamics in the X-Y plane.

The formation errors e_x, e_y, e_ψ can be expressed as:

$$\dot{e}_x = -(P_{yd} - e_y)\omega_L - v_{Fx}\cos(e_\psi) + v_{Fy}\sin(e_\psi) + v_{Lx} \tag{20}$$

$$\dot{e}_y = (P_{xd} - e_x)\omega_L - v_{Fx}\sin(e_\psi) - v_{Fy}\cos(e_\psi) + v_{Ly} \tag{21}$$

$$\dot{e}_\psi = \omega_F - \omega_L \tag{22}$$

A sliding mode control law is designed based on the formation dynamics, which makes the errors stay close to zero. Considering the dynamics of the formation error:

$$\dot{\chi} = F(\chi) + G(\chi)V \tag{23}$$

$$\chi = \begin{bmatrix} e_x \\ e_y \\ e_\psi \end{bmatrix}, \quad V = \begin{bmatrix} v_{Fx} \\ v_{Fy} \\ \omega_F \end{bmatrix} \tag{24}$$

$$F(\chi) = \begin{bmatrix} e_y\omega_L + v_{Lx} - \omega_L P_{yd} \\ -e_x\omega_L + v_{Ly} + \omega_L P_{xd} \\ e_\psi \end{bmatrix} \tag{25}$$

$$G(\chi) = \begin{bmatrix} -ce_\psi & se_\psi & 0 \\ -se_\psi & -ce_\psi & 0 \\ 0 & 0 & 1 \end{bmatrix} \tag{26}$$

Given the condition that the matrix $G(\chi)$ is full rank, the switching function can be written as:

$$\sigma_2 = \chi + k_f \int \chi\, dt \tag{27}$$

where k_f is a variable matrix to be decided. Differentiating (27) with respect to time and on the surface $\dot{\sigma}_2 = 0$, the equivalent control can be presented as:

$$\dot{\sigma}_2 = \dot{\chi} + k_f\chi = F(\chi) + G(\chi)V_{eq} + k_f\chi = 0 \tag{28}$$

$$V_{eq} = G^{-1}(\chi)(-F(\chi) - k_f\chi) \tag{29}$$

Considering the presence of uncertainties and perturbations with the assignment:

$$\dot{\sigma}_2 = \dot{\chi} + k_f\chi = F(\chi) + G(\chi)V + k_f\chi = -LSgn(\sigma_2) \tag{30}$$

$$V = G^{-1}(\chi)(-F(\chi) - k_f\chi - LSgn(\sigma_2)) \tag{31}$$

where L is a constant, positive control parameter. Then, the discontinuous control V is obtained.

III. Image Processing Algorithm and Hardware Architecture

The objective of vision-based localization algorithm is to provide the full 6-DOF transformation information between the leader-UAV and the follower one. The image processing algorithm is divided into two parts: marker detection and pose estimation. The relative coordinates is generated by a marker detection procedure, and the relative position and angle is calculated by using a pose estimation algorithm. Our outdoor experimental setup consists of two multi-rotor craft, which are converted to autonomous UAVs by adding a suit of sensors including GPS, an inertial measurement unit and a binocular vision system. Fig. 3 shows the hardware architecture and the integrated formation control system.

A. Marker Detection and Pose Estimation

The marker detection process is implemented when the markers can be seen clearly in the field of view, which means the follower-UAV is close enough to the leader-UAV. Then, a color image retrieval algorithm based on the main object region of the maker is employed. Image frames captured from the binocular camera system are mapped from the RGB space to the HSV space. It has been tested that color features detection in HSV space have enough accuracy and can be used in different backgrounds, especially in the presence of strong interfering targets. The hue and saturation channels are selected for the threshold segmentation to achieve binary images. The undesired noise in binary images can be excluded with morphology methods such as the erosion and dilation operators. After the morphological operators, the quantity of connected regions is counted as the number of feature points. The centroid of each connected region is also calculated as the image coordinate of each feature point.

In order to estimate the relative position and angle of between the leader-UAV and the follower-UAV, extracted feature points are matched to actual markers to obtain the index number of each feature point. The Munkres algorithm [15] is employed to calculate the Euclidean distance matrix between two image coordinates. After indexing these feature points, binocular pose estimation algorithm based on the LHM algorithm [16] is adopted to obtain the relative position and angle. The binocular LHM algorithm extends the original one by minimize the object-space collinearity errors of two cameras. The solution can be obtained by the use of the same iteration method as what is implemented in the original LHM algorithm. In general, the binocular LHM algorithm can converge within a small iteration beginning with any range of initial conditions.

B. *Hardware Architecture*

We used the open-source *arducopter* autopilot that can dramatically reduce design and development time, and this autopilot also provides us with an existing architecture of a development toolbox, ground station, communication protocol, and community support.

The octorotor S1000 from DJI technology Inc has been used as the leader-UAV platform. The octorotor carries a 6 cell 15000 mAh LiPo battery which powers eight brushless motors, the flight time of this customized UAV is about 15 minutes. Its maximum takeoff weight will be about 11kg by adding our suit of sensors including GPS, inertial measurement unit, mini PC, image transmission system, and the binocular vision system. The follower-UAV is designed based on the quadrotor X650 pro from XAIRCRAFT Technology Co., Ltd. Both of the UAV platform can be flown by a human pilot via an RC transmitter as backup inputs, and they also receive control signals from on-board computer simultaneously.

A visual sensor is utilized on board to obtain in-flight visual information. The binocular camera system consists of two same color video cameras. Our selection is the Mercury camera from Daheng IMAVISION, which has a compact size equipped with Mini USB 2.0 interface and has a gross weight around 100g using a 12mm lens. It can provide a resolution of up to 1292×964 pixels and 40deg field of view. The frame rate is 30 Hz, which is generally higher than that of vision algorithms (around 10 Hz).

The image processing algorithm traditionally runs on a microprocessors, but due to the high calculation precision and real-time requirements, we migrated the algorithm to an x86 computer running Linux. A separated on-board mini PC, Intel NUC, is employed to process the digitalized video signal and execute the vision algorithms. The core of our on-board PC is one of the 4th generation Intel Core i5 processors running at 1.3GHz. Equipped with a compact solid state disk, it weights around 650g. The overall vision measurement system is integrated in this vision processing computer, including marker detection, feature extraction, pose estimation and communicating with the flight controller. The position and pose data transmission between the leader-UAV and the follower-UAV is based on a pair of XBee Modules from Digi International with a UDP protocol.

The video captured by the on-board camera is transmitted and displayed in a ground station using the DJI Lightbridge 2.4G HD digital video downlink. It offers 1080p video data transmission rate up to 1.7km, while the gross weight of its on-board system is only 70g. The image transmission system is connected to the on-board computer by HDMI. The ground system can be connected to a monitor, or transmit and display the video in the ground station through a video capture board. A ground station is used to display the video captured by the on-board camera system and the position and pose data. It can provide ground operators with clear visualization during flight tests, and help operators get the real-time information of the UAVs

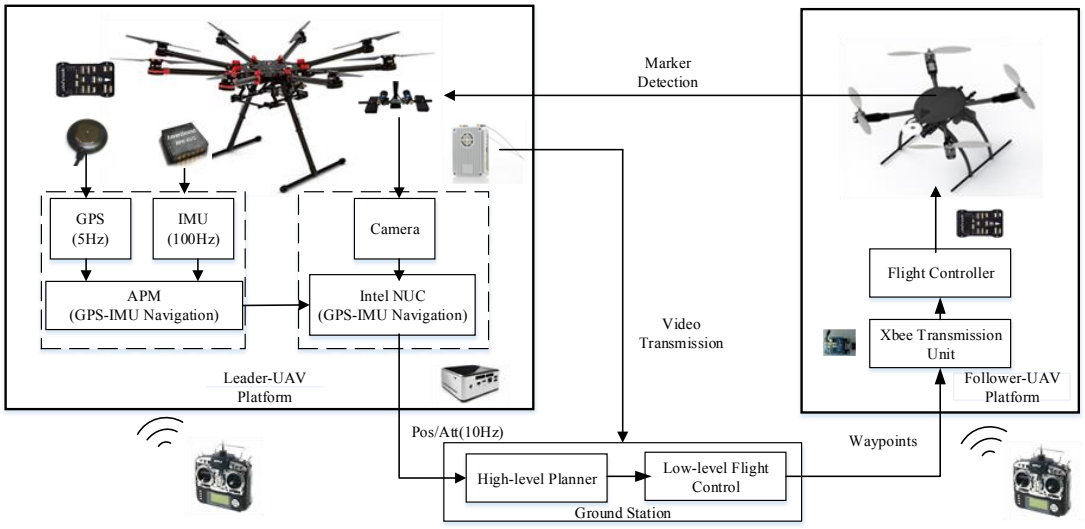

Figure 3. Hardwar architecture of our UAV platforms.

IV. Experimental Results

In order to verify that the control framework and the visual measurement algorithm proposed for leader-follower formation control, a series of outdoor experiments are conducted. Using GPS only, we are able to get close enough to have follower's markers in the field of vision of leader's camera. Then the markers would be identified in the video sequence by our binocular vision measuring system automatically. The estimated position and pose data and stitched image are also transmitted to the ground station for display. The challenge has been to get the UAV to fly a stable formation despite winds and noisy measurements from the sensors.

By applying the algorithms above, we were able to localize the follower for this 2 minute time frame for using the in-flight camera data as shown in Fig. 4. The outdoor experiment images shown in Fig. 5 are captured by the onboard computer, and the proposed visual measurement algorithm is applied. The estimated relative distances are shown in Fig. 6, which validate the performance of our algorithm with an accuracy less than 10 cm.

Figure 4. Outdoor formation control experiment based on visual measurement and IMU data.

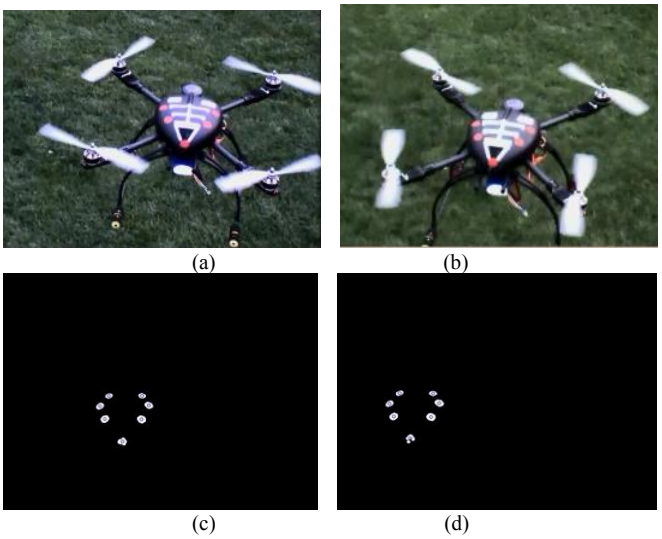

(a) (b) (c) (d)

Figure 5. Results of marker detection. (a)–(b) Cooperative makers on the follower-UAV. (c)-(d) Segmentation results of left camera and right camera, respectively.

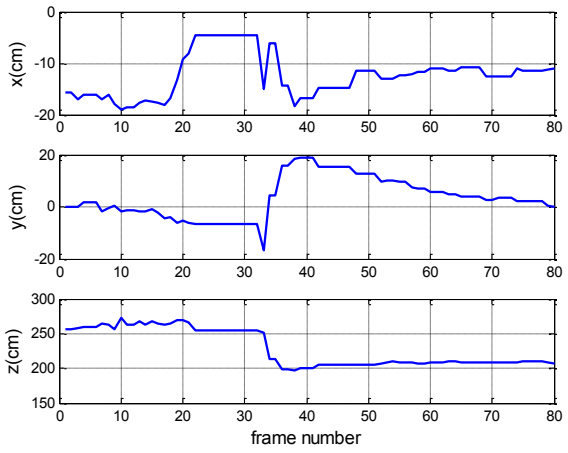

Figure 6. Relative distances between the lead-UAV and the follower-UAV.

As shown in Fig. 6, there is almost no vibration that disturbs the relative distance by integrating the position data obtained from the vision system and the IMU. However, fast maneuvers may cause the feature tracking to fail.

V. Conclusion

In this paper, a control framework to solve the leader-follower UAV formation problem in 3-D space has been presented. We stressed the need for reliable visual relative position estimation systems on UAVs to overcome the boundaries of protected lab environments. The visual estimation is based on a cooperative target detection algorithm, and the information fusion is conducted with the velocity obtained from an onboard IMU. Outdoor flight experiments are conducted to verify the effectiveness and applicability of the proposed control framework. Experimental data indicate that our visual measurement algorithm could obtain an estimation accuracy of about 5 centimeters. The experiments were also conducted to show that the proposed control method can successfully solve the formation control problem. The visual based formation control scheme presented in this paper is able to, not only solve the leader-follower formation control problem, but also solve the distributed control of complex systems, such as multi-UAV formation reconfiguration, multi-vehicle coordinate problems.

References

[1] R. W. Beard and T. W. McLain. "Multiple UAV cooperative search under collision avoidance and limited range communication constraints," in *Proceedings of 42nd IEEE Conference on Decision and Control*, vol.1, pp.25-30, 2003.

[2] N. Michael, D. Mellinger, Q. Lindsey Q, et al. "The grasp multiple micro-uav testbed," *IEEE Robotics & Automation Magazine*, vol.17, no.3, pp.56-65, 2010.

[3] F. Lin, X. X. Dong, B. M. Chen and K. Y. Lum, "A robust real time embedded vision system on an unmanned rotorcraft for ground target following," *IEEE Transactions on Industrial Electronics*, vol.59, no.2, pp.1038-1049, 2012.

[4] H. B. Duan and L. Gan, "Elitist chemical reaction optimization for contour-based target recognition in aerial images," *IEEE Transactions Geoscience and Remote Sensing*, vol.53, no.5, pp.2845-2859, 2015.
[5] A. Franchi, C. Masone, H. H. Bulthoff, et al. "Bilateral teleoperation of *IEEE/RSJ International Conference on Intelligent Robots and Systems (IROS)*, pp.2215-2222, 2011.
[6] M. Saska, V. Vonásek, T. Krajnik, et al. "Coordination and navigation of heterogeneous UAVs-UGVs teams localized by a hawk-eye approach," *IEEE/RSJ International Conference on Intelligent Robots and Systems (IROS)*, pp.2166-2171, 2012.
[7] P. Sarunic and R. Evans. "Hierarchical model predictive control of UAVs performing multitarget-multisensor tracking," *IEEE Transactions on Aerospace and Electronic Systems*, vol.50, no.3, 2253-2268, 2014.
[8] C. M. Lin, C. F. Tai, and C. C. Chung. "Intelligent control system design for UAV using a recurrent wavelet neural network," *Neural Computing and Applications*, vol.24, no.2, 487-496, 2014.
[9] N. Harl and S. N. Balakrishnan. "Impact time and angle guidance with sliding mode control," *IEEE Transactions on Control Systems Technology*, vol.20, no.6, pp.1436-1449, 2012.
[10] H. B. Duan, Q. N. Luo, G. J. Ma, and Y. H. Shi, "Hybrid particle swarm optimization and genetic algorithm for multi-UAVs formation reconfiguration," *IEEE Computational Intelligence Magazine*, vol.8, no.3, pp.16-27, 2013.
[11] C. P. Lu, G. D. Hager, and E. Mjolsness, "Fast and globally convergent pose estimation from video images," *IEEE Transactions on Pattern Analysis and Machine Intelligence*, vol.22, no.6, pp.610-622, 2000.
[12] F. Ruffier and N. Franceschini. "Optic flow regulation: the key to aircraft automatic guidance," *Robotics and Autonomous Systems*, vol.50, no.4, pp.177-194, 2005.
[13] F. Kendoul, K. Nonami, I. Fantoni, et al. "An adaptive vision-based autopilot for mini flying machines guidance, navigation and control," *Autonomous Robots*, vol.27, no.3, 165-188, 2009.
[14] N. Guenard, T. Hamel, and R. Mahony. "A practical visual servo control for an unmanned aerial vehicle," *IEEE Transactions on Robotics*, vol.24, no.2, 331-340, 2008.
[15] J. Munkres, "Algorithms for the assignment and transportation problems," *Journal of the Society for Industrial & Applied Mathematics*, vol.5, no.1, pp.32-38, 1957.
[16] C. P. Lu, G. D. Hager, and E. Mjolsness, "Fast and globally convergent pose estimation from video images," *IEEE Transactions on Pattern Analysis Machine Intelligence*, vol.22, no.6, pp.610-622, 2000.